

# VEGETATION PRODUCTIVITY IN DRYLANDS FROM MERIS FAPAR TIME SERIES

Ute Gangkofner<sup>(1)</sup>, Carsten Brockmann<sup>(2)</sup>, José Carlos Brito<sup>(3)</sup>, João Carlos Campos<sup>(4)</sup>, Per Wramner<sup>(5)</sup>, Gregor Ratzmann<sup>(6)</sup>, Rasmus Fensholt<sup>(7)</sup>, Kurt Günther<sup>(8)</sup>

<sup>(1)</sup> GeoVille Information Systems GmbH, Sparkassenplatz 2, A-6020 Innsbruck, Austria, Email: [gangkofner@geoville.com](mailto:gangkofner@geoville.com)

<sup>(2)</sup> Brockmann Consult GmbH, Max-Planck-Straße 2, D-21502 Geesthacht, Germany, Email: [carsten.brockmann@brockmann-consult.de](mailto:carsten.brockmann@brockmann-consult.de)

<sup>(3)</sup> CIBIO, Research Centre in Biodiversity and Genetic Resources of the University of Porto R. Padre Armando Quintas, 4485-661 Vairão, Portugal, Email: [jcbrito@cibio.up.pt](mailto:jcbrito@cibio.up.pt)

<sup>(4)</sup> CIBIO, Research Centre in Biodiversity and Genetic Resources of the University of Porto R. Padre Armando Quintas, 4485-661 Vairão, Portugal, Email: [jc.campos1859@gmail.com](mailto:jc.campos1859@gmail.com)

<sup>(5)</sup> Brockmann Geomatics Sweden AB, Torshamnsgatan 39 SE-164 40 Kista, Sweden, Email: [per.wramner@brockmann-geomatics.se](mailto:per.wramner@brockmann-geomatics.se)

<sup>(6)</sup> FU Berlin, Altensteinstr. 6, 14195 Berlin, Germany, Email: [gregor.ratzmann@fu-berlin.de](mailto:gregor.ratzmann@fu-berlin.de)

<sup>(7)</sup> University of Copenhagen, Øster Voldgade 10, 1350 Copenhagen K, Denmark, Email: [rf@ign.ku.dk](mailto:rf@ign.ku.dk)

<sup>(8)</sup> DLR German Aerospace Center, Münchener Straße 20, D-82234 Wessling, Germany, Email: [Kurt.Guenther@dlr.de](mailto:Kurt.Guenther@dlr.de)

## ABSTRACT

This paper provides an overview of the European Space Agency (ESA) DUE Project Diversity II, specifically the dryland component of this dual project with a dryland and an inland water part. The 10 years of MERIS data have been exploited using full and reduced resolution fAPAR data to profile and trace the vegetation development in 22 dryland sites all over the globe. Objectives were to map and assess status and trends of vegetation productivity and express the results in a suite of indicators. The work was driven by the information needs of the CBD (Convention on Biological Diversity) and the UNCCD (UN Convention to Combat Desertification).

## 1. INTRODUCTION

With the Diversity II project ESA aims at contributing to the strategic goals of two UN conventions: the Convention on Biological Diversity (CBD), and the UN Convention to Combat Desertification (UNCCD). As unanimously confirmed in a user and expert Diversity II dryland workshop held in Bonn in July 2014 [1], both conventions have a common denominator in terms of basic information needs: vegetation productivity. Diversity II exploits data of the MERIS sensor on board ENVISAT from June 2002 until April 2012. As major proxy of vegetation productivity, MERIS based full resolution (FR) and reduced resolution (RR) fAPAR data (Fraction of Absorbed Photosynthetically Active Radiation) were derived and processed to half-monthly time series data. According to [2], fAPAR is the index “most directly related to loss of plant productive capacity” and it is the core variable used in models of primary production in terrestrial ecosystems. Hence, fAPAR was considered an appropriate biophysical

variable to represent status and trends of vegetation productivity.

A total of 22 dryland areas were selected ranging from 0.42 to 1.64 Mio km<sup>2</sup> and covering an overall area of 15.7 Mio km<sup>2</sup> (Fig. 1). The dryland sites were selected among WWF ecoregions with an aridity index (ratio of mean annual precipitation to mean annual potential evapotranspiration) largely from 0.05 to 0.65 [3]. Further criteria were the global distribution and representativeness for major terrestrial dryland ecosystems, and the inclusion of several regions of primary biodiversity importance.



Figure 1. Distribution of Diversity II dryland sites

The work resulted in so called first order and second order indicator maps showing average vegetation conditions of the observation period, trends, and epochal changes. A total of 43 first order, seven second order and three phenology products were generated per test site, amounting to 1166 map products overall<sup>1</sup>. A product user handbook [4] provides an overview and

<sup>1</sup> Diversity II products, i.e. data and documents including site-specific booklets and the Product User Handbook (PUH) [4] can be downloaded at <http://www.diversity2.info/products/>

interpretation examples of the derived products. It presents also NOAA GIMMS (Global Inventory Modeling and Mapping Studies [23]) NDVI (Normalized Difference Vegetation Index) based results derived with the same methodology for longer time periods reaching back as far as 1982 and comparisons of the latter to MERIS fAPAR based indicators.

The generated status and trend maps were contrasted with faunal species abundance data derived from models and partly from in situ investigations in test sites 10, 12, 13, 15, and 20. Results are also described in [4].

## 2. MATERIALS AND METHODS

### 2.1. Input data

MERIS fAPAR data derived with the JRC (Joint Research Center) algorithm [5] from both MERIS FR (300m) and RR (1200m) data were the major data source in all 22 test sites. They were processed to half-monthly time series data using maximum composites. For comparison with the MERIS fAPAR based results, MERIS (FR/RR) NDVI data [6] were evaluated in site 4 (Northern Kazakhstan) and site 12 (Southern Africa West). For the same sites, modeled NPP (Net Primary Productivity) data (1km) generated by DLR with BETHY/DLR [7], [8]<sup>2</sup> were provided and also compared to the fAPAR derived results. TRMM 3B42 data with a spatial resolution of 0.25° were summed to half-monthly rainfall values, and beyond 50° N and S, GPCP v2p2 rainfall (2.5°) were used in order to relate vegetation greenness to rainfall. CCI Soil Moisture data 2.0 (0.25°) served as additional source for water availability. NOAA GIMMS3g NDVI [23] data were used for trend comparisons with the fAPAR based results and for demonstration of longer term developments.

The rainfall and soil moisture data were integrated or respectively interpolated to half-monthly values, with a grid spacing of  $\approx 0.07273^\circ$  (8 km at the equator), and geographic coordinates (WGS84) to match the GIMMS NDVI data. GlobCover (2009) data served as reference information for map generation (water mask) and CCI (2010) land cover data were contrasted with some Diversity II products in [4]. The MERIS based fAPAR and NDVI data and the rainfall and soil moisture data were generated and respectively pre-processed with ESA BEAM.

### 2.2. Methods

The Diversity II methodology for drylands is based on the extraction of phenological and productivity parameters of the vegetation. The entire processing from

the initial gap filling of the fAPAR (and NDVI) data to the final product generation was developed and implemented as a fully automated processing chain with the Spatial Modeler of ERDAS IMAGINE. State of the art methods for the extraction of phenological and productivity parameters, (e.g., [9], [10]) were partly applied. In some points, additional or alternative features were developed as described below.

#### *Data gap filling*

Where possible, data gaps in the MERIS FR derived fAPAR data were filled with the RR based fAPAR data, whose acquisition was more frequent, keeping the FR pixel size of 300m\*300m. Gaps not closed this way were largely filled with a two-sided linear trend extrapolation approach. For extrapolation, the weighted slope between three neighbors of the gap on its two sides (prior and after) was used. Data gaps of only one value were linearly interpolated. This way, gaps up to five half-monthly values were filled in an iterative procedure. No smoothing was applied to the input data except for derivation of the Start of Season (SoS) as described below.

#### *Concept of vegetation phenology and productivity*

Fig. 2 presents the developed concept of the parameterization of phenology and productivity using a location in South Africa at (Y -29.896337, X 25.7373764 [dd]). The diagram displays the temporal course of the MERIS fAPAR data during a 3-year period and the subdivision into different seasonal periods. The **vegetation year** includes the full yearly vegetation cycle starting after the end of the preceding **dry season** (and/or cold season) and ending at the end of the following **dry season** (and/or cold season) – or in case of several green seasons during a year – at the beginning of the most frequently observed green season in the monitoring period. The **vegetation year** can be subdivided into different seasons, limited by defined starting and ending points in time. The **growing season** includes the major vegetation peak(s), i.e. ascending and descending parts of the time series and starts once a selected greenness threshold is surpassed (the first time) on the way from the start of the vegetation year to the green peak. This threshold is depicted as brown dotted line and labeled with “**baseline**” in the phenology diagram. Hence, an explicit difference between the start of the vegetation year and the start of the vegetation season is made. The **dry season** (brown parts of the fAPAR curve) starts once the baseline is surpassed. The **growing season length** is the time span between the start and the end of the growing season, marked with horizontal light green arrows in Fig. 2. The **growing season amplitude** is the span between the baseline and the **greenness maximum** of the vegetation year.

In Fig. 2, the second vegetation year has a very short growing season, which does not include the first small peak. Not including such small peaks into the growing

<sup>2</sup> The data have been kindly provided by Kurt Günther and Markus Tum, DLR

season was deliberately decided in order to make the “length of the growing season” indicator sensitive to years with shorter main vegetation seasons.

#### Calculation of Start of Season (SoS)

The SoS is the key phenological parameter, which provides access to many further phenological properties. Yet, it is differently defined and calculated by different authors with consequently deviating results, as demonstrated by [11].

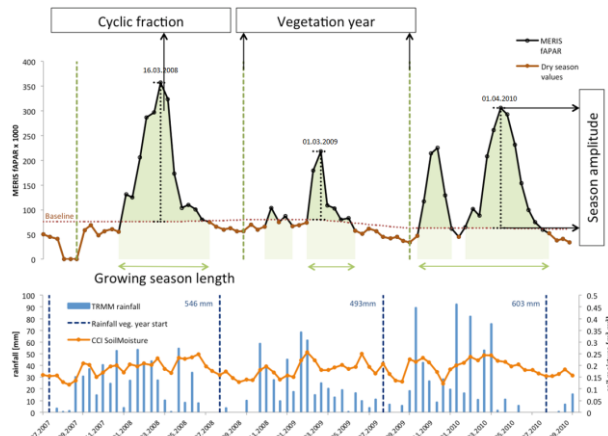


Figure 2. Scheme of the extracted phenological and productivity parameters, and corresponding rainfall and soil moisture data.

In the Diversity II test sites a wide range of SoS conditions is met including sharp to weak increases of the vegetation signal, big to very small and hardly recognizable vegetation peaks, unimodal vegetation curves and multiple SoS per year, and all combinations of the above. In addition, the timing of the SoS can significantly vary between years.

In order to automatically cope with all global conditions, a method sensitive to any increase in the vegetation curve was developed in order to minimize the number of missed SoS. At the same time, SoS of vegetation peaks considered too small or of too short duration were discarded by respective fine-tuning of the method. Prior to the derivation of the SoS, low outliers (> 5% of the difference of Max and Min of three years) of the input data were linearly interpolated. The following three-step procedure was applied:

1. First, for each year, the timing of all potential SoS was derived based on the cumulative gradients of the fAPAR (or NDVI and NPP) time series. The moving sums of six consecutive increments were derived, which create peaks prior to vegetation peaks, whose temporal position and size were used to determine the SoS. By means of further fine-tuning, the SoS was defined to occur right at the start of the respective vegetation increase period. It was derived for the years from 2003 to 2011, for which full MERIS coverages were available.

2. In the second step, the temporal ranges of the most frequent SoS accumulations during these nine years were determined. The starts of season within these ranges (of each year) were taken as the “dominant” SoS group, which constitutes the local start of the vegetation year. In cases where no SoS had been derived for a given year or several years within the determined range, the mean SoS of the other years was used for substitution. This way, isolated SoS (not occurring in temporal clusters) could be discarded, and missing SoS in extremely dry years substituted. In regions with two (or more) growing seasons per year, in many cases not all of their SoS were detected in all years. Consequently, within one of the resulting temporal SoS ranges, the number of SoS derived was higher than in the other(s). This SoS group constituted the dominating SoS group. If two SoS groups were detected in the same number of years, the first within the calendar year was taken as the dominant SoS.
3. In the third step, the time series of (corresponding) SoS were smoothed in the following way: the mean of the SoS of the previous and following years was derived for each SoS, and the SoS of a particular year was replaced by this mean if the timing of the mean was earlier than the SoS actually determined. This way, the often strong SoS fluctuations from year to year could be avoided, and the length and timing of the vegetation years equalized.

#### Definition of the baseline

Besides the SoS, the “baseline” is a crucial parameter in the presented concept of vegetation phenology and productivity, as it separates dry (or cold) season values from the cyclic vegetation and determines the amount of the “cyclic vegetation”, as well as the size of the “amplitude”. Conceptually, the baseline was defined as the upper boundary of the often considerably fluctuating dry season values. The aim was to get baselines with smooth transitions between vegetation years, in order to make the derived productivity values comparable from year to year. The procedure was adapted towards this concept and is described in [4].

#### Derivation of the pheno-productivity parameters

Once the SoS and the baseline are determined, the remaining parameters can be derived in a rather straight forward way (on a pixel basis). The “vegetation year” constitutes the time frame for all other parameters, i.e. it is used for temporally referencing all further phenological parameters derived from the vegetation time series data. A wealth of parameters was calculated, even though not all of them were used for generating the Diversity II products. Parameters not used for Diversity II products include for instance the number and timing of vegetation peaks within the vegetation year, the time of the maximum and the maximum value itself, or the amplitude. All these are interesting

parameters, were saved, and can be activated for additional analyses and the generation of further products. However, to keep the number of products manageable, the focus was laid on the three basic vegetation periods and their productivity values:

- Vegetation year and corresponding average values;
- Cyclic vegetation and corresponding sum values;
- Dry season and their average values.

The yearly average reflects a property which may be called “overall level of greenness of the vegetation year”. Theoretically it expresses the standing green biomass, where perennially green vegetation occurs, plus the net primary productivity. The cyclic vegetation (see Fig. 2) can be understood as the total amount of green biomass produced during the growing season(s), i.e., a proxy more directly related to the yearly NPP. The dry/cold season average is a measure for the amount of live vegetation outside the main rainy season (or respectively the major vegetation peak). The derived Diversity II products concentrate on these three parameters and their relations, which are considered to express major functional vegetation properties at a regional scale.

#### *Extraction of rainfall and soil moisture data*

Quite obvious in Fig. 2 is the time shift between rainfall and the onset of vegetation development, often amounting to +/- two months. For this reason, the period for the extraction of rainfall sums corresponding to a vegetation year was shifted back by two months. Soil moisture was extracted with a time back-shift of only one month, as it could be frequently observed to react to rainfall with a delay of +/- one month. Rainfall and soil moisture were extracted for the entire vegetation years, and for the growing season. In the second case, the same shifts were applied, but the extraction period ended at the end of the growing season.

#### *Derivation of RUE and SMUE parameters*

Rain Use Efficiency (RUE) was defined by [12] as *quotient of annual primary production by annual rainfall*. RUE thus expresses the amount of biomass growing per unit rainfall water. Theoretically, soil moisture is more directly related to plant water availability than rainfall, so SMUE (Soil Moisture Use Efficiency) is offered as a potentially useful additional indicator. Both RUE and SMUE were derived for the vegetation year, the dry season and the cyclic vegetation, using rainfall sums and soil moisture averages integrated over the vegetation year and the growing season, respectively.

RUE has been widely applied as an indicator for human induced land degradation or improvement, but also challenged for several reasons. These are discussed for instance by [13], [14] or [15]. One of the main issues is that RUE is correlated to a spatially and temporarily varying degree with rainfall, for which it is supposed to

normalise. Thus RUE (or SMUE) trends will partially reflect trends of water availability and can be expected to not consistently indicate human caused land degradation. The also tested RESTREND method [16], [17] delivered somewhat different results than RUE. It is also based on not (consistently) applying assumptions [15], [17], and has not been used in the Diversity II product generation.

#### *Product generation*

All products refer to the eight vegetation years worldwide covered by the MERIS data. The start of the vegetation years ranges globally from January 2003 until December 2010, depending locally on the average timing of the dominant SoS group and the individual yearly SoS within this SoS range. The original fAPAR (and NDVI) values have been multiplied by 1000 and these values were used for the map legends of the products as well. The final status, trend, and change products have been generated with discrete and globally consistent classes and color schemes, making them comparable across all test sites. The status products express the eight year averages of vegetation productivity (of vegetation years, cyclic vegetation and dry season), RUE and SMUE, and their coefficients of variation for these eight years.

Trend products were calculated for the same parameters applying the Theil-Sen trend (TS) median slope trend analysis [18], [19]. TS is especially suited for short and noisy time series [14]. Statistical trend significance was tested with a Mann-Kendall significance test [20], [21], using  $p = 0.9$ .

In addition to these “*first order status and trend products*”, phenology and “*second order*” products were derived. Second order products are combinations of two to three first order indicators, and address two themes: The first is “functional biodiversity” with the indicator: “*Functional Classes*”, which are expressed by a combined classification of vegetation year productivity and the percentage of cyclic vegetation of the yearly vegetation (see [4] for details). Both a status and an epochal change indicator were generated for the functional classes, supplemented with a trend relation indicator differentiating seasonal vegetation productivity trends. The second theme addressed by the second order indicators is the “assumption-free” combination of rainfall and vegetation productivity trends. For this purpose, a group of indicators called “*Direct relation between Rainfall and Vegetation Productivity Trends*” was conceived. These indicators show where rainfall and vegetation trends go in the same direction, where they exhibit opposite trends, or where rainfall trends do not lead to vegetation response of the productivity parameters.

In addition, the following phenology parameters were turned into products in Diversity II: Median of the dominant SoS, average start of the growing season, and the length of the growing season. SoS and the start of



the growing season (see Fig. 2) were both included in the product suite, as they span the period when different scholars define – or different methods derive the “start of season”. The start of the growing season, for

instance, corresponds conceptually to the SoS derived by the commonly used Timesat software [9], depending on the parameter setting with regard to the definition of the cyclic vegetation.

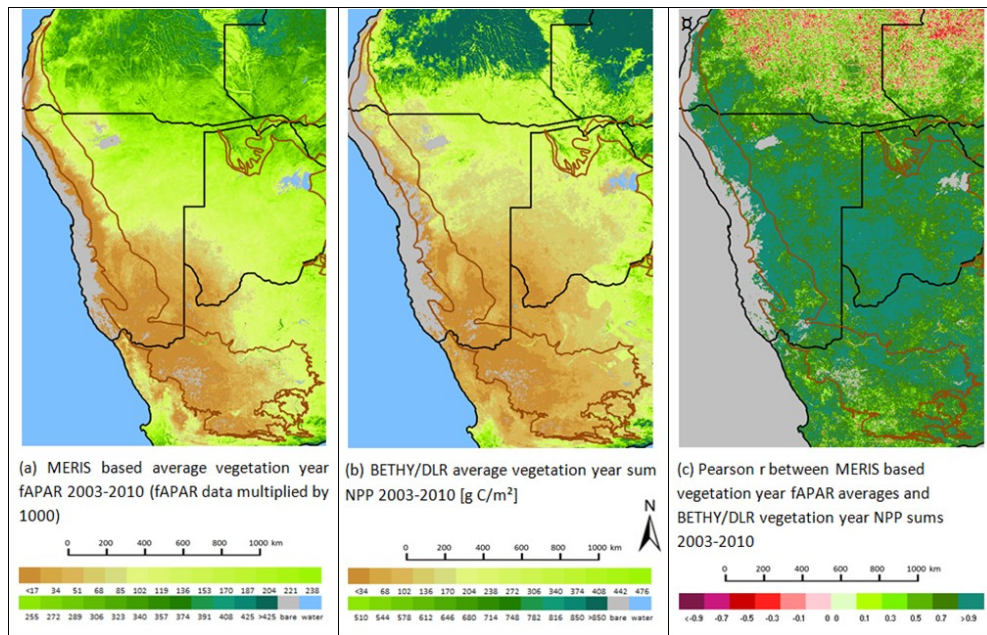


Figure 3. Comparison of MERIS fAPAR based yearly greenness (a) versus modelled NPP (b), and correlation between both (c), Diversity II test site 12, Southern Africa West

### 3. RESULTS

A comprehensive overview and description of the resulting products and their potential usages is provided in [4]<sup>1</sup>. More individual information to each test site is found in so-called booklets<sup>1</sup>. A few examples of the use cases and cross-comparisons of the results to those derived by other authors or with other data presented in [4] are summarized below.

In two test sites, the developed processing chain was applied to modelled NPP data, derived with BETHY/DLR [7], [8]. Among many other input data, the BETHY/DLR modelling results were derived with SPOT VEGETATION based LAI (Leaf Area Index) data and GLC 2000 land cover data. The NPP (vegetation year) and the MERIS fAPAR based results were compared. In Fig. 3 the fAPAR based vegetation year average greenness is contrasted with the 8 year yearly NPP sum modelled with BETHY/DLR for test site 12, Southern Africa West, and a map of Pearson’s r between the yearly values is shown in the right. While the general patterns of vegetation productivity fit well, especially in regions with higher NPP in the north (Angola) the two maps show discrepancies and even negative correlations between the yearly values. Low to medium positive correlations are found within the arid southern part of the actual test AOI (brown polygon). The scattergram of the eight year mean fAPAR and the

NPP average sums is illustrated in Fig. 4, showing a logarithmic relation and a high positive correlation with an  $r^2$  of 0.89. In [4] further results of the comparison are shown, i.e. RUE average and trends and NPP (proxy) trends.

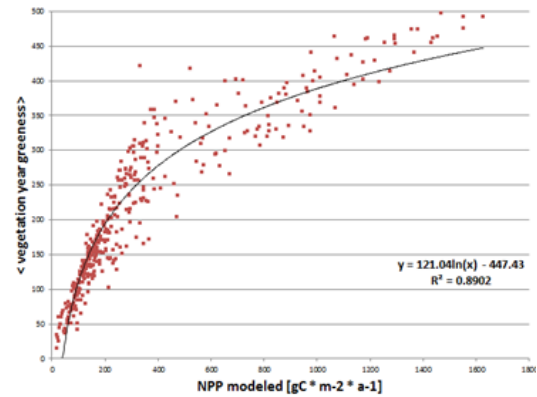


Figure 4. Vegetation year average (fAPAR based) greenness versus modelled NPP (vegetation year sum) for test site Southern Africa West

Due to the relatively high NPP values in the North, also the average RUE is relatively high with the modelled NPP data, compared to the fAPAR based RUE. Thus, the variation of RUE can be subject to quite strong discrepancies depending on the NPP parameterisation.

The same comparison results are presented for site 4 (Northern Kazakhstan) in [4], showing good correspondence and, in this case, a linear correlation between modelled NPP and fAPAR ( $r^2=0.83$  for vegetation year averages).

Another comparison was conducted between MERIS fAPAR and NDVI data for the same two test sites. SoS differences and the Pearson's  $r$  between the vegetation year averages of fAPAR and NDVI are displayed in Fig. 6, again for site 12 (Southern Africa West). The upper left map shows the differences between the fAPAR and the NDVI based SoS. Underneath a detail

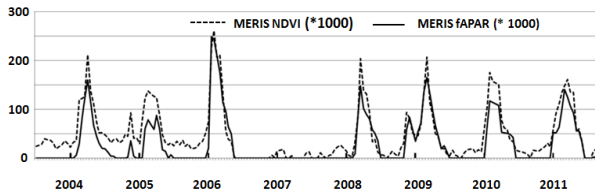


Figure 5. MERIS NDVI and MERIS fAPAR time series in Namibia, at X: 18.65197380, Y: -24.09031143 [dd].

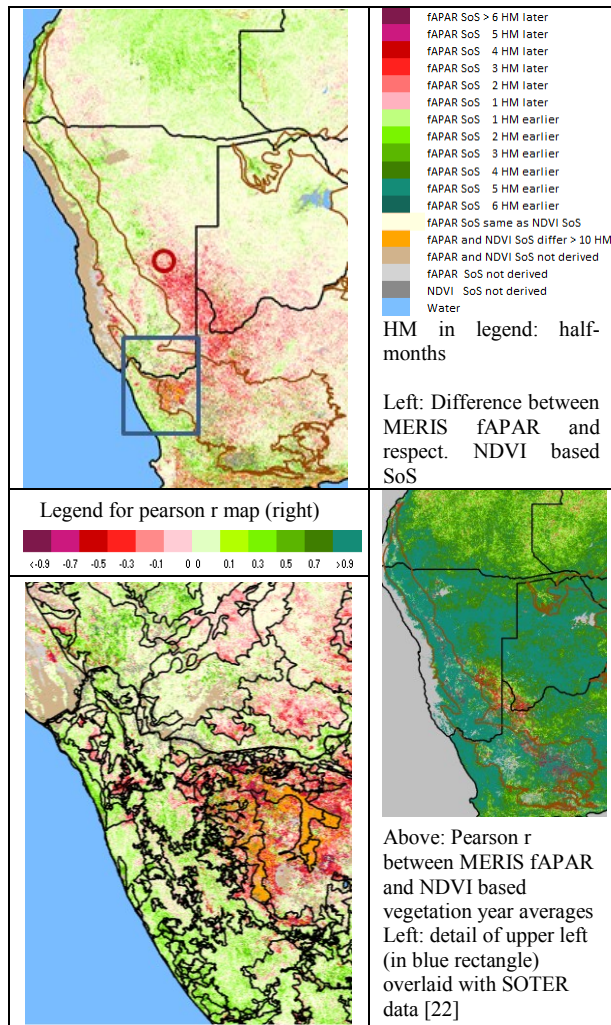


Figure 6. Comparison of MERIS fAPAR and NDVI based results in site 12, Southern Africa West

of the latter is shown, overlaid with SOTER data (Soil and Terrain data [22]). The partly substantial SoS differences are often aligned with the soil and terrain units of SOTER. The orange area in the SoS difference map, which exhibits de-correlated SoS, seems to overlay exactly on an area of Kalahari dune fields of distinctive red sand. Surrounding areas tend to have a less sandy yellow soil, so potentially impact the NDVI and the fAPAR less. Fig. 5 contrasts the MERIS fAPAR and the NDVI values for a pixel within the red circle indicated in Fig. 6, upper left, during the course of the eight vegetation years. While the fAPAR values (solid line) go down to zero during the dry season, the NDVI hardly reaches the bottom and partly exhibits an earlier rise of the values after the dry season than fAPAR. In a part of the area with a strong SoS delay of the fAPAR to the NDVI (red areas in Fig. 6, upper left map), also the correlation coefficient between their vegetation year averages are low and partly negative. These areas have TRMM precipitation means (2003-2010) around 250mm and more, significantly higher than the regions further to the West and Northwest with higher correspondence between fAPAR and NDVI. Consequently, soil colour patterns and vegetation cover have a combined influence on the consistency of the

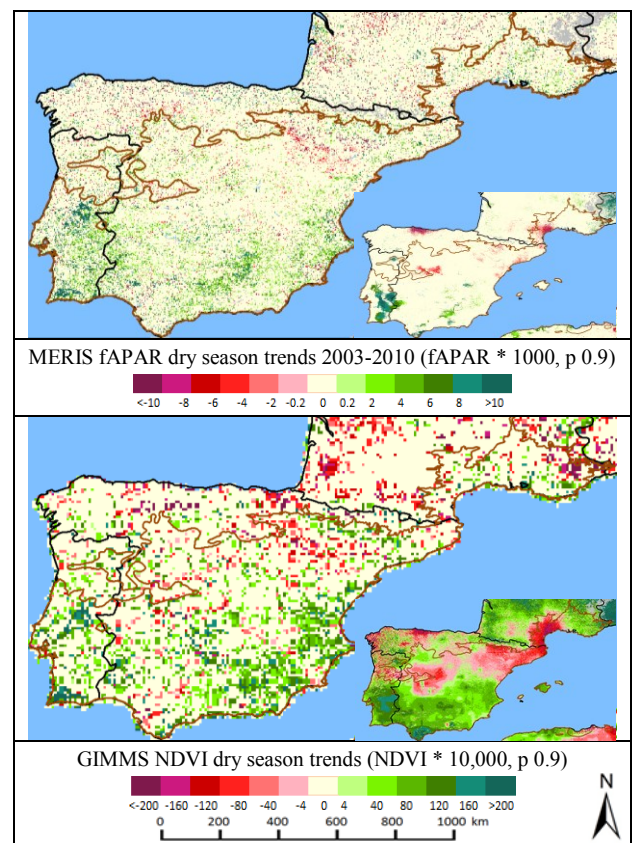


Figure 7. MERIS fAPAR dry/cold season vs. NOAA GIMMS NDVI dry/cold season trend slopes 2003-2010 with rainfall trends (upper right) and epochal rainfall differences (lower right)



NDVI and fAPAR in these regions. In some areas/years (orange areas, Fig. 6, left) the NDVI exhibits substantial response even though the fAPAR has zero values.

Consistency of the MERIS fAPAR derived trends with other results has been thoroughly studied and presented in [4]. MERIS fAPAR and especially NOAA GIMMS NDVI derived trends were compared for all three seasonal integration periods for various test sites. In general, the trends were found comparable with few exceptions, even though derived with TS for MERIS fAPAR versus OLS (ordinary least square) trends for GIMMS data. Fig. 7 contrasts MERIS fAPAR and GIMMS NDVI dry season trends for southern Europe, showing widespread trend similarities. The patterns of epochal rainfall differences, shown in the lower right of Fig. 7 (differences of the rainfall means of the vegetation years 2003-2006 and 2007-2010) are largely similar, and correspond only in the north (SW France) to trends of the cyclic vegetation, as shown in [4].

Methods applied to isolate NPP proxy developments from variations in water availability in order to identify potential degradation or improvements have been shortly addressed in section 2.2. Soil moisture was used for this purpose in addition to rainfall, resulting in often quite obvious discrepancies between RUE and SMUE (examples are shown in the dryland booklets<sup>1</sup> for all test sites). The second order indicator group “*Direct relation between Rainfall and Vegetation Productivity Trends*” was conceived as a quasi-assumption-free alternative to RUE (or RESTREND). An example is shown in Fig. 8 for test site 22, Eastern Mediterranean Countries.

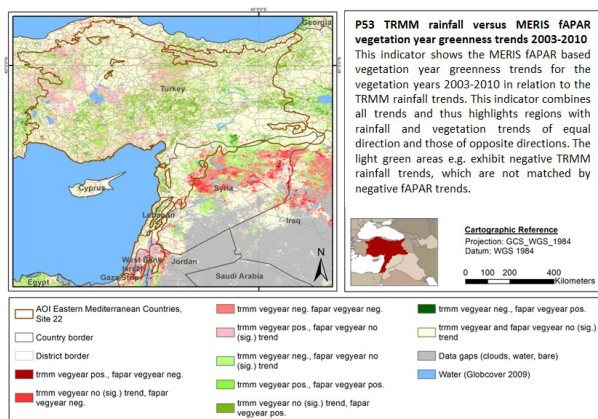


Figure 8. TRMM rainfall vs. MERIS fAPAR based vegetation year greenness trends 2003-2010

Such a trend relation map exhibits areas where NPP proxy trends occur with or without rainfall trends (and vice versa) and may have other reasons than water quantities, such as temperature changes or anthropogenic causes. In addition, we found that quite often vegetation trends reflect epochal rainfall differences and not only (significant) rainfall trends. This supports the memory effect of vegetation response

to rainfall variations [24], [25] and further challenges strict year by year analysis of vegetation productivity and water availability (see also [15]).

A last example of the Diversity II results is given in Fig. 9, showing a map of the second order product “*Functional Classes*”. These originate from a combined classification of the average greenness of the vegetation year and the percentage of cyclic vegetation of the yearly vegetation. The numbers in the legend increase with increasing values of these parameters. The lighter the tone, the higher is the percentage of the cyclic vegetation and the lower the share of woody and herbaceous evergreen vegetation. The resulting maps are being shown to be closely related to land use/cover patterns and to soil and terrain type and structures in [4]. The functional classes are considered to deliver valuable information on the patterns of productivity and the phenological composition of the dryland vegetation, which are important properties of vegetation vigour and functional biodiversity.

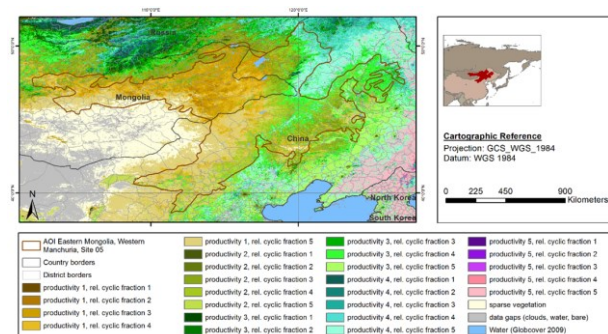


Figure 9. Functional classes, test site 05, Eastern Mongolia-Western Manchuria

#### 4. CONCLUSIONS

The dryland component of the ESA Diversity II project focused on information needs of the CBD and UNCCD, exploiting the full archive of ENVISAT MERIS data. Map products based on vegetation phenology and productivity parameters (NPP proxies), in combination with data of water availability have been generated, describing vegetation status and trends from 2003 to 2011. The resulting products should be analysed in integrated approaches along with information from longer periods and finer spatial scales, and caution due to the short observation period. The developed methods are applicable to other vegetation time series data, such as NDVI or modelled NPP data. More comprehensive project conclusions can be found in [4].

#### REFERENCES

1. ESA DUE Project DiversityII: 2<sup>nd</sup> Dryland User Consultation Meeting (2014). Downloadables at: <http://www.diversity2.info/ucm/ucm2d/>

2. GEO BON (2011). Adequacy of Biodiversity Observation Systems to support the CBD 2020 Targets. A report prepared by the Group on Earth Observations Biodiversity Observation Network (GEO BON), for the Convention on Biological Diversity.
3. UNEP (United Nations Environment Programme). (1997). *World atlas of desertification* 2ED. London, UK: UNEP.
4. ESA DUE Project DiversityII (2015). *Product User Handbook - Dryland*.
5. Gobron, N. (2011). Envisat's Medium Resolution Imaging Spectrometer (MERIS) Algorithm Theoretical Basis Document: FAPAR and Rectified Channels over Terrestrial Surfaces. JRC Scientific and Technical Reports.
6. Günther, K.P., Maier, S. (1999). AVHRR compatible NDVI ATBD. DLR document ID: MAPP-ATBD-NDVI.
7. Wißkirchen, K., Tum, M., Günther, K.P., Niklaus, M., Eisfelder, C., Knorr, W. (2013). Quantifying the carbon uptake by vegetation for Europe on a 1km<sup>2</sup> resolution using a remote sensing driven vegetation model. *Geosci. Model Dev.*, 6, 1623–1640.
8. Tum, M. (2012). Modelling and validation of agricultural and forest biomass potentials for Germany and Austria. Dissertation, Georg-August-Universität Göttingen.
9. Eklundh, L., Jönsson, P. (2012). *Timesat 3.1 Software Manual*.
10. Ivits, E., Cherlet, M., Mehl, W., Sommer, S. (2013). Ecosystem functional units characterized by satellite observed phenology and productivity gradients: A case study for Europe. *Ecological Indicators* 27, 17–28.
11. White, M.A., De Beurs, K.M., Didan, K., Inouye, D.W., Richardson, A.D., Jensen, O.P., O'Keefe, J., Zhang, G., Nemani, R.R., Van Leeuwen, W.J.D., Brown, J.F., De Wit, A., Schaepman, M., Lin, X., Dettinger, M., Bailey, A.S., Kimball, J., Schwartz, M.D., Baldocchi, D.D., Lee, J.T., Lauenroth, W.K. (2009). Intercomparison, interpretation, and assessment of spring phenology in North America estimated from remote sensing for 1982–2006. *Global Change Biology* 15(10), 2335–2359.
12. Le Houérou, H.N. (1984). Rain use efficiency: a unifying concept in arid-land ecology. *Journal of Arid Environments*, 7, 213–247.
13. Fensholt, R., Rasmussen, K. (2011). Analysis of trends in the Sahelian 'rain-use efficiency' using GIMMS NDVI, RFE and GPCP rainfall data. *Remote Sensing of Environment* 115, 438–451.
14. Fensholt, R., Rasmussen, K., Kaspersen, P., Huber, S., Horion, S., Swinnen, E. (2013). Assessing Land Degradation/Recovery in the African Sahel from Long-Term Earth Observation Based Primary Productivity and Precipitation Relationships. *Remote Sensing*, 5, 664–686.
15. Ratzmann, G., (2014). *EO-based Relationships Between Vegetation and Rainfall in Drylands. Towards better understanding of eco-hydrological patterns and dynamics*. Master's thesis at the Faculty of Science, University of Copenhagen.
16. Wessels, K.J., Prince, S.D., Malherbe, J., Small, J., Frost, P.E., VanZyl, D. (2007). Can human-induced land degradation be distinguished from the effects of rainfall variability? A case study in South Africa. *Journal of Arid Environments* 68, 271–297.
17. Wessels, K.J., Van den Bergh, F., Scholes, R.J. (2012). Limits to detectability of land degradation by trend analysis of vegetation index data. *Remote Sensing of Environment*, 125, 10–22.
18. Theil, H. (1950). A rank-invariant method of linear and polynomial regression analysis I, II and III, *Nederl. Akad. Wetensch. Proc.*, 53, 386–392, 521–525, 1397–1412.
19. Sen, P. K. (1968). Estimates of regression coefficients based on Kendall's tau. *J. Amer. Statist. Assoc.* 63, 1379–1389.
20. Mann, H.B. (1945). Non-parametric tests against trend. *Econometrica*, 13, 163–171.
21. Kendall, M.G. (1962). *Rank Correlation Methods*, Charles Griffin and Company, London.
22. Soil and Terrain Database for Southern Africa (ver. 1.0) (SOTERSAF).
23. Tucker, C.J., Pinzon, J.E., Brown, M.E. (2004). Global Inventory Modeling and Mapping Studies. NA94apr15b.n11-VIg, 2.0, Global Land Cover Facility, University of Maryland, College Park, Maryland, 04/15/1994.
24. Zhou, Y. (2013). *Inter-annual memory effects between Soil Moisture and NDVI in the Sahel*. Master's Thesis at the Department of Physical Geography and Ecosystem Science of Lund University.
25. Martiny, N., Richard, Y., Camberlin, P. (2005). Interannual persistence effects in vegetation dynamics of semi-arid Africa. *Geophysical research letters*, 32(24).